JOINT INSTITUTE FOR NUCLEAR RESEARCH

Dzhelepov Laboratory of Nuclear Problems

FINAL REPORT ON THE INTEREST PROGRAMME

Radiation Protection and the Safety of Radiation Sources

Supervisor:

Dr. Said Abou El-Azm

Participant:

Bosquit Glyssa May

University of Debrecen

Participation period:

February 13 – March 26, Wave 8

Dubna, 2023

Abstract

Radiation protection has been implemented following an increase in activities related to ionizing radiation. Radiation protection reduces radiation doses, minimizes the negative effects of ionizing radiation, increases awareness of radiation risks, and avoids unsafe practices. The foundation for radiation protection regulations and protocols has been laid by this initiative.

Important parameters for radiation protection and safe handling of radioactive sources are at the heart of this project's work. The tasks were successfully completed using various software including ROOT, Origin Analysis, Excel and SRIM simulation, based on test data obtained in the laboratory.

Finally, we compare the technical data of the BGO and NaI detectors. Unknown sources are identified using the equation of the calibration line with known energy. The attenuation coefficients of aluminum and copper, and the range of alpha particles in air are determined.

1. Introduction

Radioactivity is a phenomenon existing in the universe and natural radiation sources are peculiar attributes of the environment. Radioactivity is the spontaneous release of energy or particles when an unstable atom transforms into a stable state. And these energy or particles are known as radiation. Radiation can be classified as ionizing and non-ionizing, depending on its ability to penetrate matter. Ionizing radiation can detach electrons from atoms or molecules and alters the atomic level when interacting with matter, including living things. This type of radiation includes alpha particles, beta particles, neutrons, gamma rays, and x-rays, which can damage body cells, organs, and even cause death in high doses. Whereas, non-ionizing radiation is a lower energy radiation, that can make the molecules vibrate resulting to production of heat. This type of radiation includes microwave, UV light, radio waves, and infrared light. [1],[2],[3]

In a tale of paradox, radiation can be deadly, but it also saves lives. Radioactive sources play a major role in medicine, energy production, industry, agriculture, space exploration, and law enforcement, to name a few. In its correct uses and doses, and necessary safety precautions, ionizing radiation can be utilized beyond measure. Parallel to these applications, the workers, the public, and the environment may be exposed to radiation risks, which should be assessed and controlled, if needed. Therefore, activities that involve the use of ionizing radiation in medicine, the operation of nuclear installations, the production and transport of radioactive material, and the management of radioactive wastes must be subject to safety standards. These concerns prompted the development of radiation protection, which aims to reduce unnecessary radiation exposure and minimize the harmful effects of ionizing radiation. [1],[2],[4]

The main objective of this project is to establish a solid foundation for radiation protection and radiation sources. Additionally, provide the necessary practical skills and basic tools for those interested in working in the field of radiation protection and the safe use of radiation sources through a series of laboratory works.

2. Background

2.1. Sources of Radiation Exposure

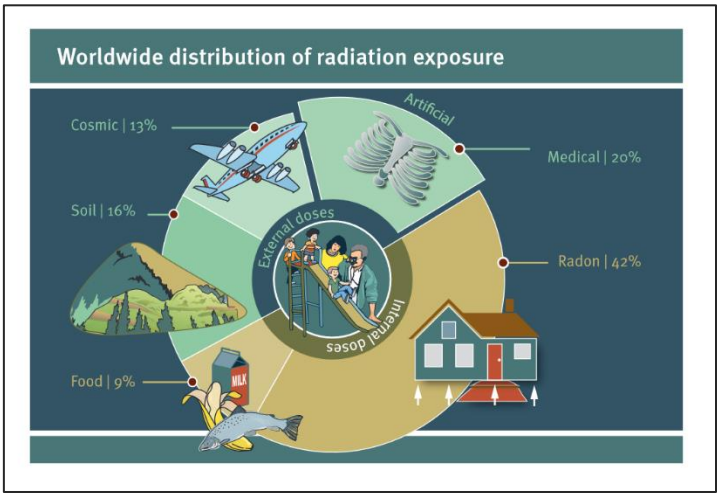

Figure 1: Worldwide distribution of radiation exposure. Retrieved from: UNEP

Radiation surrounds humans constantly and can be categorized into two: natural background radiation and artificial radiation. Three sources of natural background radiation are cosmic radiation (in space), terrestrial radiation (in the nature), and internal radiation (in the body). On the contrary, artificial radiation is emitted due to human activities such as nuclear weapon testing, application of radiation in medicine, consumer products, and others. There are two distinct groups exposed to artificial or man-made radiation: members of the public and occupationally exposed individuals. For regulatory purposes, radiation protection is addressed for different groups.

Based on the chart data above published by United Nations Environment Programme (UNEP), approximately 80% of human exposure originates from natural sources, and 20% is a result of artificial sources, mainly from radiation application in medical procedures. [5],[6]

Radiation exposure can also be characterized based on their path of irradiation. Radioactive substances and radiation in the environment may irradiate the human body *externally*. Or an individual may inhale the substances in air, swallow them in food and water, or absorb them through skin, and then irradiate the body *internally*. Doses from external and internal exposure are similar, as considered globally. [6]

2.2. Radiation Units

When ionizing radiation hits the human body or objects in general, energy is deposited. The absorbed energy from exposure is termed as “dose”. The dose quantities of radiation can be defined in several ways, depending on the nature and strength of the radiation source, biological sensitivity

of the exposed area, and exposure parameters such as time, distance, and shielding. The most used dose measurements are absorbed dose, equivalent dose, and effective dose.

a. Absorbed dose describes the energy imparted by radiation in a unit mass of material, such as tissue or organ. It is expressed in grays (Gy).
b. Equivalent dose is the absorbed dose multiplied by the radiation factor (W_R), which accounts for the differences in effect depending on the type of radiation. It is expressed in sieverts (Sv).
c. Effective dose is the equivalent dose multiplied by organ factors (W_T), which accounts for the susceptibility to harm and the differences in sensitivity among organs. It is also expressed in sieverts (Sv). [6],[7]

2.3.Principles of Radiation Protection

The International Commission on Radiological Protection (ICRP) made recommendations about basic frameworks for radiation protection, which intended to protect human health and the environment. Through this initiative, the fundamental principles of radiation protection have been established, highlighting on “justification”, “optimization”, and “application of dose limits”.

Justification: The act of using radiation or any other activity that alters the radiation exposure situation should be allowed only if the benefits outweigh the radiation risks. This applies to three different situations: emergency exposure, existing exposure, and planned exposure.

Optimization: When benefits of using radiation outweigh the radiation risks, all doses should be kept as low as reasonably achievable (ALARA), while considering the economical and societal factors. To promote this principle, dose constraints and reference levels are employed.

Application of dose limits: The total dose to any individual from regulated sources in planned exposure should not exceed the indicated appropriate limits. This is commonly specified in two ways: occupational exposure (50 mSv per year and 100 mSv per five years) and public exposure (1 mSv per year). Dose limits do not apply to medical exposure since it can hinder the patients from receiving the necessary treatment.[8]

3. Experimental Set-up and Methods

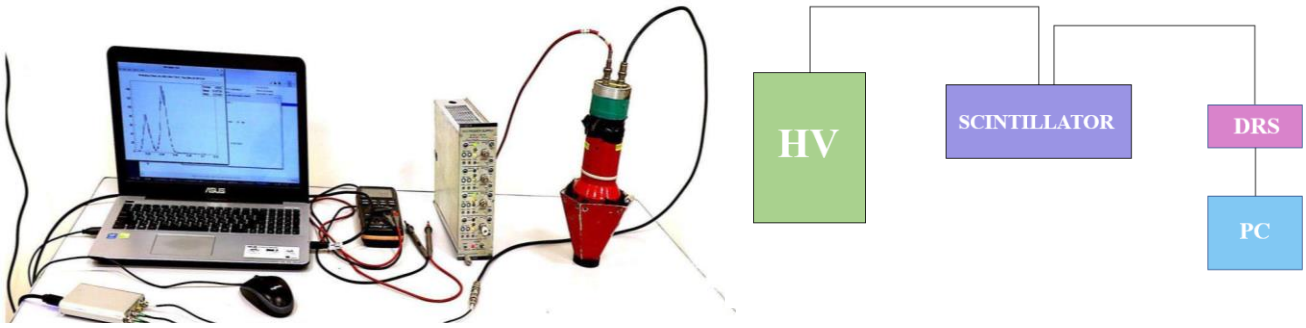

Figure 2: Experimental Laboratory Set-up

3.1. Scintillator Detectors and Photomultiplier Tube (PMT)

3.1.1. Scintillator Detectors

A scintillator produces sparkles of light (scintillation), when excited by ionizing radiation. Scintillates are well-known as one of the oldest types of radiation detectors and measurements could be made with photographic films. In the modern designs, a scintillation detector is coupled with an amplifying device such as a photomultiplier tube (PMT), which can convert the scintillations into electrical pulses. These pulses are analyzed and counted electronically to obtain information about the radioactive source.

Inorganic crystals and organic scintillators are two commonly used scintillators. In inorganic crystals scintillators, the scintillation mechanism is dependent on the crystal lattice structure. While in organic scintillators, the fluorescence mechanism emanates from transitions in the energy levels of a single molecule and fluorescence can be detected independently from the physical state of the molecule. There are different scintillating materials used such as inorganic crystals, organic crystals, organic liquids, plastic scintillators, noble gases, and scintillating glass. [9]

The experimental results analyzed in this project mainly came from two inorganic scintillator detectors: BGO and NaI (Tl). Other data were collected from a plastic detector and a pixel detector.

Scintillator properties of crystals

Scintillator	Light output	Decay (ns)	Wavelength (nm) max	Density (g/ cm2)	Hygroscopic
Na(Tl)	100	250	415	3.67	yes
CsI	5	16	315	4.51	slightly
BGO	20	300	480	7.13	no
BaF2(f/s)	3/16	0.7/630	220/310	4.88	slightly
CaF2	50	940	435	3.18	no
CdWO4	40	14000	475	7.9	no
LaBr3(Ce)	165	16	380	5.29	yes
LYSO	75	41	420	7.1	no
YAG(Ce)	15	70	550	4.57	no

FYS-KJM5920 - Nuclear Measurement Methods and Instrumentation 9

Figure 3: Basic properties of scintillating crystals

a. **BGO Detectors – Bismuth Germanate ($Bi_4Ge_3O_{12}$)**

BGO detector is a remarkably efficient gamma-ray absorber with a good peak-to-total ratio, resulting from the high values of its atomic number, density, and Z. It is a characteristically hard, rugged, and non-hygroscopic crystal which neither cleaves nor exhibits significant self-absorption of the scintillation light. BGO has a diverse application such as Positron Emission Tomography (PET), Compton suppression spectrometers, geological logging, and special roles in space and medical physics. [10],[11]

b. **NaI (Tl) Detectors – Sodium Iodide (Thallium-doped)**

Sodium Iodide crystals have an inordinate scintillation efficiency and available in single-crystal and polycrystalline form (with varying sizes and geometries), making it the most extensively used scintillator. It has a high level of optical output, no significant absorption of scintillation light, and capable of detecting gamma rays of low and intermediate energies. Thallium-doped Sodium Iodide detectors produce one of the highest signals in a PMT per amount of radiation absorbed. These detectors have a variety of applications such as Time-of-Flight (ToF) measurements, positron lifetime studies, PET, and special roles in nuclear and high energy physics. [11],[12]

3.1.2. Photomultiplier Tube (PMT)

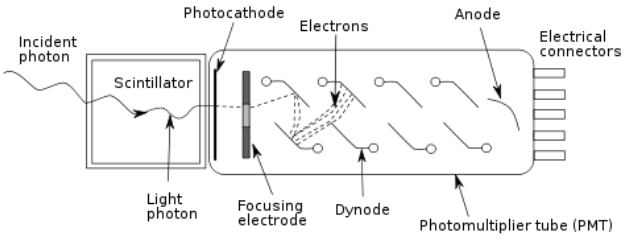

Figure 4: Schematic diagram of a scintillator detector coupled with PMT

Scintillator detectors essentially consist of a scintillator material, coupled with a photodetector (either PMT or photodiode) that can convert the scintillation light into electrical signals.

Photomultiplier tubes are the commonly employed photodetectors, which are composed of a photocathode accompanied by a series of dynodes. When light hits the photocathode, photoelectron is emitted and focused onto the first dynode. Electrons are produced which then strike a chain of dynodes, dislodging more electrons all the way to the anode where the amplified signal is collected. This electrical signal is proportional to number of photoelectrons. [13]

3.2. Tasks

Task 1: Relation between the Resolution and Applied Voltage for BGO detectors

The energy resolution of a detector refers to its ability to separate signals or peaks and accurately determine the energy of the incoming radiation. The better the energy resolution, the finer it can distinguish two adjacent energy peaks, allowing the identification of different decays or radionuclides in the spectrum. The resolution is calculated from the peak at full width half maximum (FWHM) divided by the location of the peak centroid, H_0:

$$Resolution = \frac{\sigma}{Mean} * 2.35 \quad (1)$$

Applied Voltage (V)	Mean	Sigma	Resolution (%)
1200	1.624	0.441	63.815
1300	1.378	0.264	45.022
1400	1.923	0.283	34.584
1500	2.996	0.437	34.277
1600	4.410	0.614	32.719
1700	6.102	0.765	29.462
1900	10.669	1.218	26.828
2000	13.662	1.500	25.801

Table 1: Resolution (%) of BGO detector corresponding to the applied voltage.

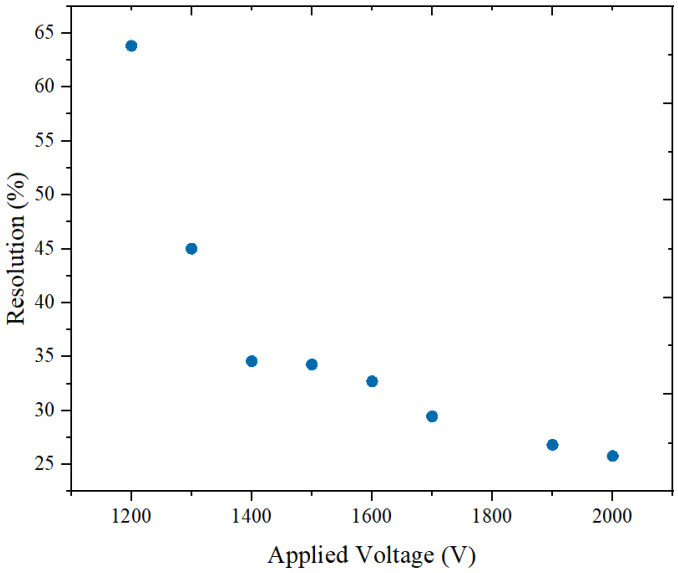

Figure 5: The relation between the resolution and applied voltage for BGO detector.

In detectors, energy resolution is expressed as a percent of the FWHM of a specific energy. If the percent value is lower, the better is the energy resolution.

The obtained plot indicates that the higher the applied voltage, the better the energy resolution.

Task 2: Energy Calibration of BGO detectors at 2000V

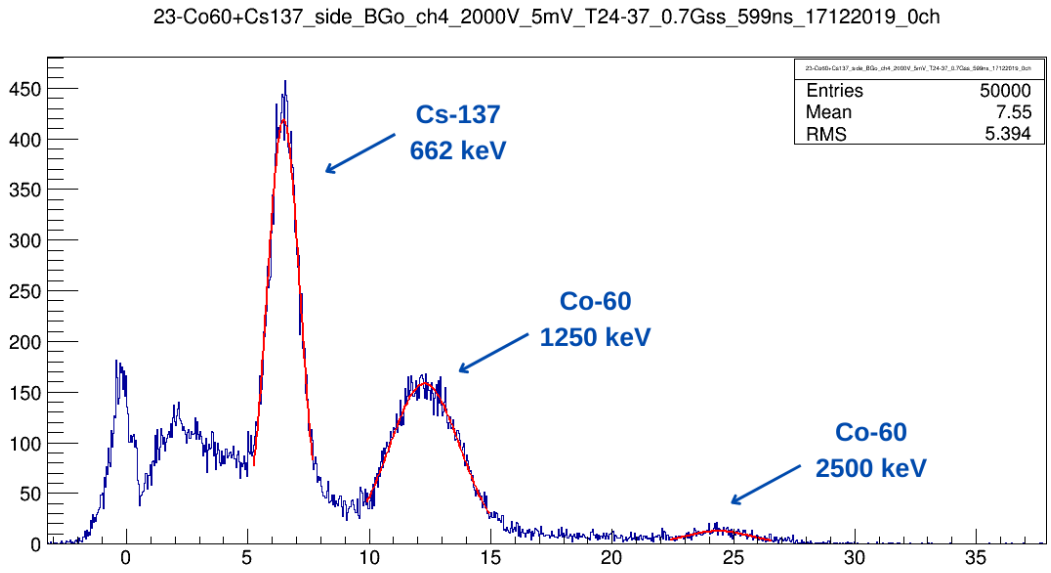

Figure 6: The energy spectrum of Cs-137 and Co-60 from BGO detector measurements at 2000V.

The channel number (mean) is obtained by making a Gaussian fit using the ROOT software. From the plot of energy vs. channel number (mean), a calibration curve is made, and the equation of the line is generated.

Isotope	Channel	Energy (keV)
Cs-137	6.475	662
Co-60	12.279	1250
	24.379	2500

Table 2: Channel and energy of Cs-137 and Co-60 peaks from a BGO detector.

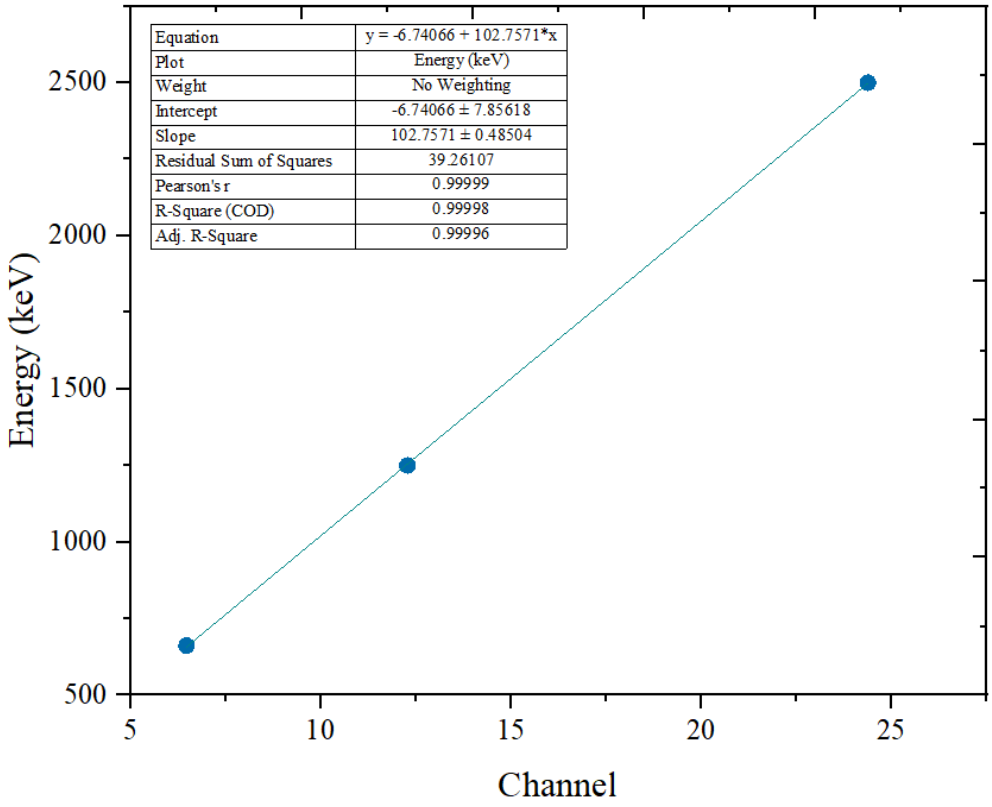

Figure 7: Energy calibration function for Cs-137 and Co-60 spectrum from BGO detector measurements.

The equation of the energy calibration line for BGO detector is:

$$y = 102.7571x - 6.74066$$

Where:

x = channel number (mean),

y = energy of the peaks (in keV)

2.1. Identification of Unknown Sources

For the identification of the energy spectrum and its unknown sources, the following steps can be applied:

i. Using the ROOT software, a Gauss function is fitted into the spectrum of the unknown energy, and the channel number (mean) is obtained.

ii. From the equation of the calibration line of BGO detector, the channel number can be converted to energy.

iii. The unknown source of the calculated energy can be determined using the Nuclide Datasheet.

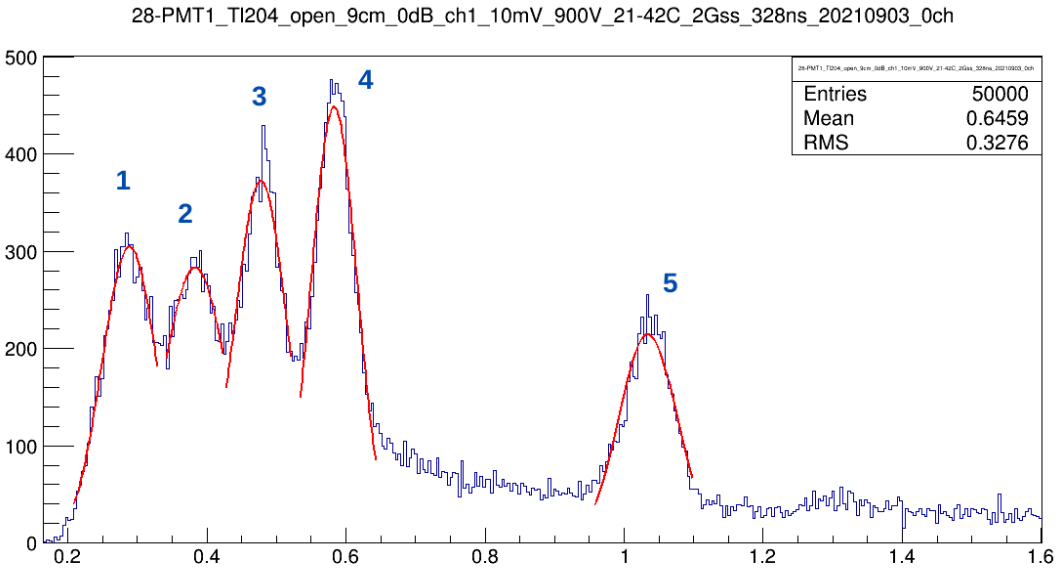

Figure 8: Energy spectrum of the unknown sources from BGO detector measurements at 900V.

Peak	Channel	Energy (keV)	Energy (MeV)	Peak ID
1	0.289	22.956	0.022956	**Sm-151**
2	0.383	32.615	0.032615	**Mg-28**
3	0.478	42.377	0.042377	**Rh-103m** or **I-129**
4	0.583	53.167	0.053167	**Rh-104m** or **Te-132**
5	1.034	99.510	0.099510	**Gd-153** or **Au-145**

Table 3: Energy, channel, and peak ID of the unknown sources identified using the Nuclide Datasheet.

Sample Calculation (Peak 1):

Equation of the calibration line: $\boldsymbol{y = 102.7571x - 6.74066}$ **;** and $\boldsymbol{x = 0.289.}$

Substitute the value of x:

$$y = 102.7571 * 0.289 - 6.74066$$

$$y = 22.956 \text{ keV}$$

Task 3: Relation between the Resolution and Applied Voltage for NaI detectors

Applied Voltage (V)	Mean	Sigma	Resolution (%)
900	23.670	0.635	6.304
1000	40.655	0.966	5.584
1100	65.792	1.514	5.408
1200	98.707	2.032	4.838
1300	137.347	2.616	4.476

Table 4: Resolution (%) of NaI detector corresponding to the applied voltage, derived from mean and sigma using equation (1).

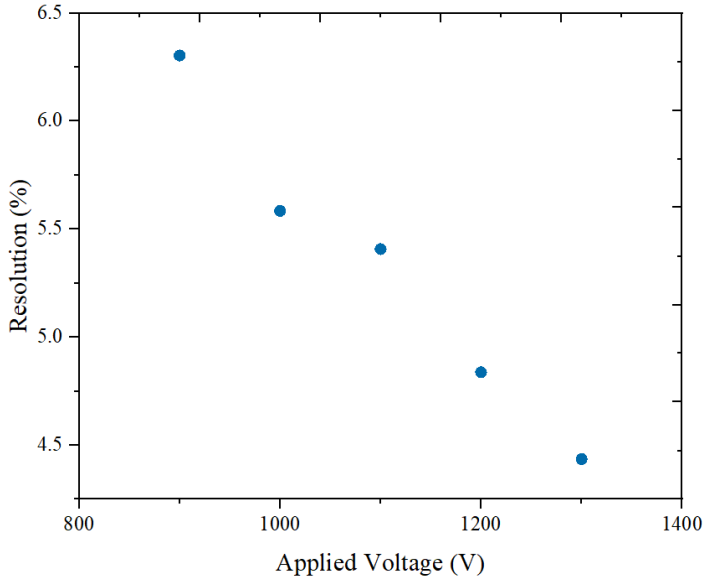

Figure 9: The relation between the resolution and applied voltage for NaI detector.

The obtained plot indicates that the higher the applied voltage, the better the energy resolution, like BGO detectors.

But in contrast, NaI detectors have a higher and more favorable resolution than BGO detectors. Comparing the applied voltage, BGO has a resolution of 25.801% at 2000V, while NaI has a resolution of 4.476% at 1300V.

Task 4: Energy Calibration of NaI detectors at 800V

An NaI detector has more light output, so its resolution is twice as good as a BGO detector. It can separate the two peaks of Co-60 with energies of 1170 keV and 1330 keV, respectively. This is the reason that four peaks are visible instead of three, in the energy spectrum below.

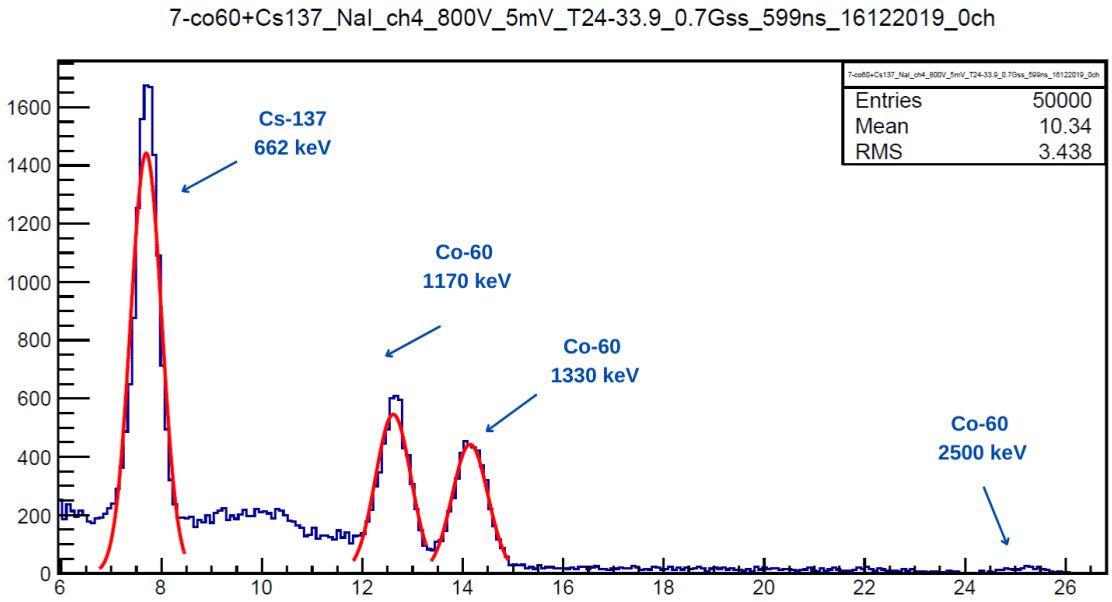

Figure 10: The energy spectrum of Cs-137 and Co-60 from NaI detector measurements at 800V.

Isotope	Channel	Energy (keV)
Cs-137	7.696	662
Co-60	12.624	1170
	14.145	1330
	25.199	2500

Table 5: Channel and energy of Cs-137 and Co-60 peaks from an NaI detector.

Similarly, the channel number (mean) is obtained by making a Gaussian fit using the ROOT software. The channel and the energy of each peak is given on the table above. The energy is plotted against the channel number, and a calibration curve is fitted into it. From this, the equation of the generated calibration line for NaI detector is:

$$\mathbf{y = 105.18685x - 153.46699}$$

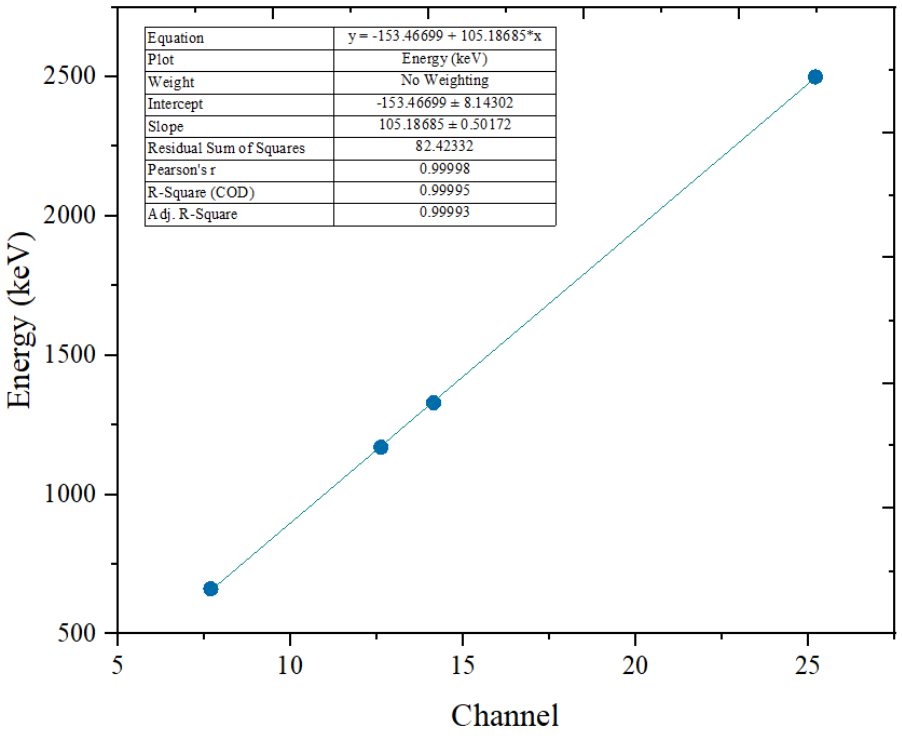

Figure 11: Energy calibration function for Cs-137 and Co-60 spectrum from NaI detector measurements.

4.1. Identification of Unknown Sources

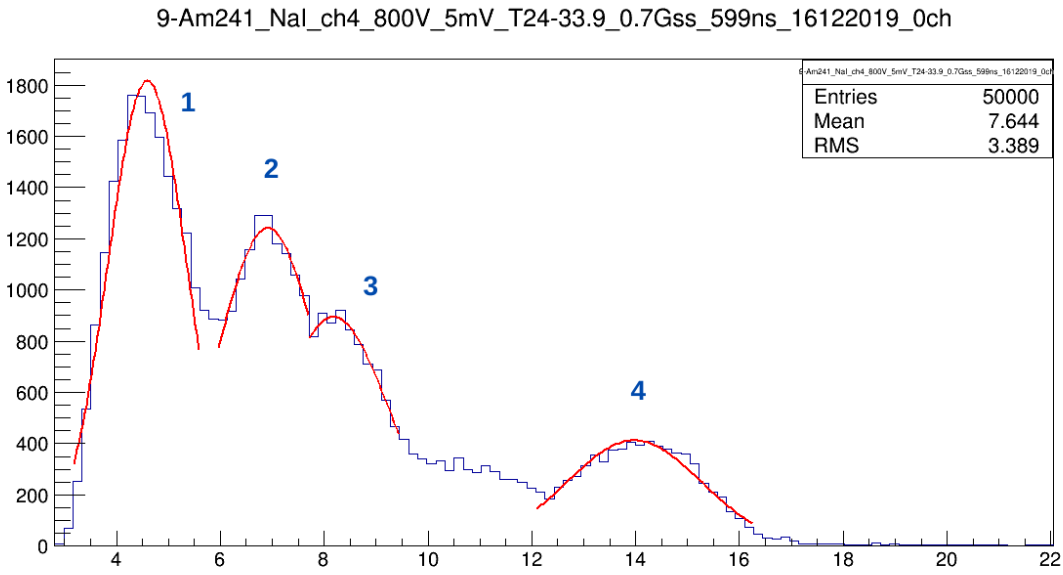

Figure 12: Energy spectrum of the unknown sources from NaI detector measurements at 800V.

Peak	Channel	Energy (keV)	Energy (MeV)	Peak ID
1	4.593	329.656	0.32966	**Ir-194**
2	6.915	573.900	0.57390	**Bi-207**
3	8.178	706.751	0.70675	**Tc-129m**
4	13.973	1316.309	1.31631	**Ca-47**

Table 6: Energy, channel, and peak ID of the unknown sources identified using the Nuclide Datasheet.

Sample Calculation (Peak 1):

Equation of the calibration line: $\mathbf{y = 105.18685x - 153.46699;}$ and $\boldsymbol{x = 4.593.}$

Substitute the value of x:

$$y = 105.18685 * 4.593 - 153.46699$$

$$y = 329.656 \text{ keV}$$

Task 5: Determination of the attenuation coefficient

Every material has its unique attenuation coefficient. Linear attenuation coefficient (μ) is a constant that describes the fraction of attenuated (absorbed or scattered) incident photons in a beam per unit thickness of a material. This covers all possible interactions such as coherent scattering, Compton scattering, and photoelectric effect. Linear attenuation coefficient can be calculated from the following formula:

$$I = I_0 e^{-\mu x}$$

Where:

x = absorber thickness,

I = intensity transmitted through an absorber of thickness x,

I_0 = intensity at zero absorber thickness,

μ = linear attenuation coefficient.

Linear attenuation coefficient has two main features: increases as the atomic number and physical density of the absorbing material increases, and it decreases with increasing photon energy (except at K-edges). Its variant is the mass attenuation coefficient, which is defined as a normalization of

the linear attenuation coefficient per unit density of a material, resulting in a value that is constant for a given element or compound. [14]

Experimental Equipment:

- Detector: BGO detector
- Voltage: 2000V
- Radioactive source: Cs-137, $E_{Cs} = 662\ keV$
- Attenuation material: Aluminum and Copper

5.1. Attenuation coefficient of Aluminum (Al)

Thickness (cm)	I/I_0
0	1
0.15	0.75573
0.3	0.71623
0.45	0.70569
0.75	0.68596
0.9	0.67155
1.08	0.66103
1.26	0.63939

Table 7: Al thickness necessary to reduce the intensity of a beam to the desired level.

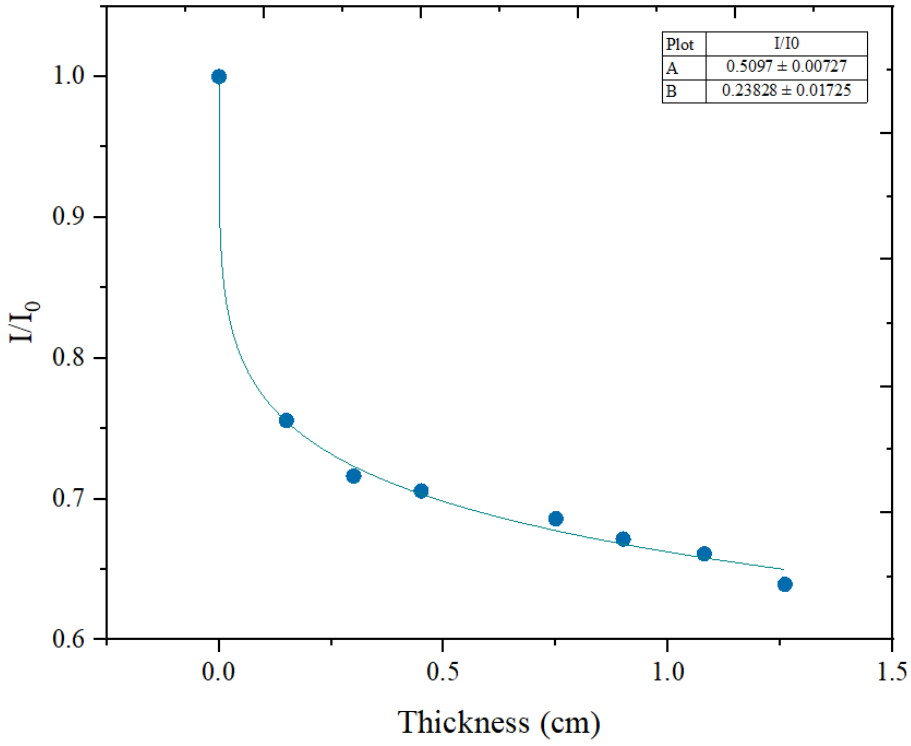

Figure 13: Determination of linear attenuation coefficient of Al using BGO detector with Cs-137 as the radioactive source.

From the non-linear fitting curve in Origin Analysis, the obtained linear attenuation coefficient of aluminum (Al) is: ***0.23828 ± 0.01725 cm^{-1}***.

5.2. Attenuation coefficient of Copper (Cu)

Thickness (cm)	I/I_0
0	1
0.2	0.73931
0.25	0.7357
0.4	0.68065
0.8	0.58611
1	0.53827
1.2	0.48042

Table 8: Cu thickness necessary to reduce the intensity of a beam to the desired level.

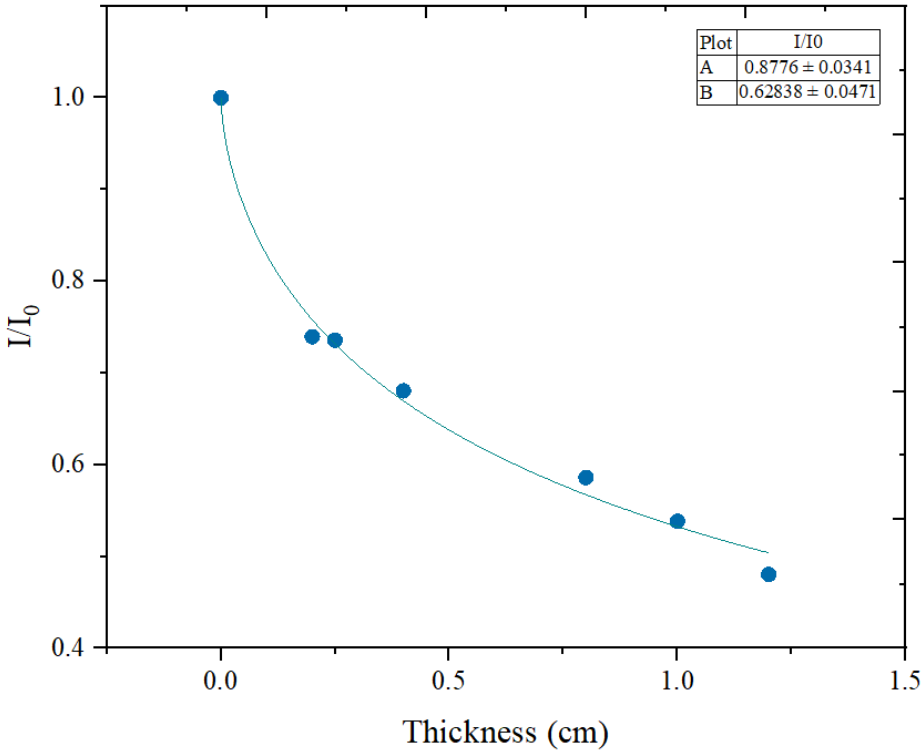

Figure 14: Determination of linear attenuation coefficient of Cu using BGO detector with Cs-137 as the radioactive source.

From the non-linear fitting curve in Origin Analysis, the obtained linear attenuation coefficient of copper (Cu) is: ***0.62838 ± 0.0471 cm^{-1}***.

Task 6: Range of Alpha Particles in Air

Range is characterized as the path length that a particle travel from its source through matter, before it is stopped. It is influenced by the type of particle, its original kinetic energy, and the medium through which it travels. Range is especially important for charged particles, like electrons and alpha particles. Alpha particles particularly travel in almost straight lines because they are thousands of times heavier than atomic electrons, to which they lose energy slowly. Their range is usually measured in a straight line from the source to the point where ionization stops. [15]

In this experiment, plastic detector is used instead of a BGO detector. This is because BGO detector has a thin aluminum foil layer and shielding can occur, leading to energy loss and inaccurate measurements.

Experimental Equipment:

- Radioactive Source: Pu-239
- Energy of He: 5.5 MeV
- Detector: Plastic Detector
- Voltage: 2000V

Distance (cm)	Counts/sec
0	440
0.5	390
1	360
1.5	340
2	320
2.5	300
3	280
3.5	260
3.8	260
4	260

Table 9: Number of counts per second of source at different distances from the detector.

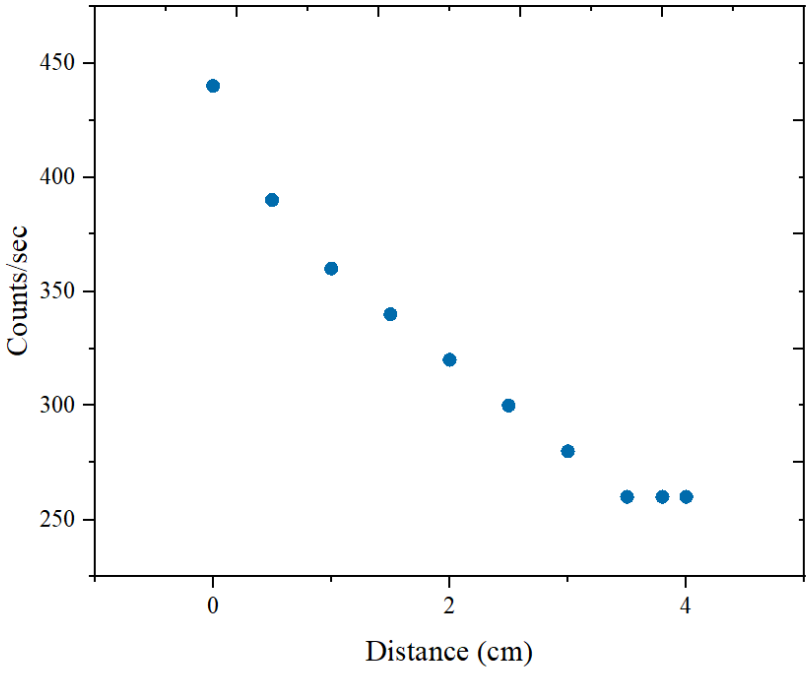

Figure 15: The range of alpha particles from plastic detector measurements at 2000V and Pu-239 radioactive source (5.5 MeV).

From the table and the plot, it can be observed that the counts per second decreases as the distance increases, until reaching a point where the number of counts is constant. It means that there is no more signal detected. Therefore, the range of alpha particles in air is about ***3.5 cm***.

6.1. Range of Alpha Particles in Air by SRIM Simulation (Monte Carlo)

Using the SRIM software, it is possible to observe the simulation of the total path length traveled by alpha particles in air. Two plots are obtained: the depth vs. y-axis and the ionization (Bragg peak/curve) of the alpha particles. The Bragg curve represents the energy loss rate as a function of the distance through a stopping medium. The Bragg peak is the maximum, and beyond that, the energy deposition drops sharply.

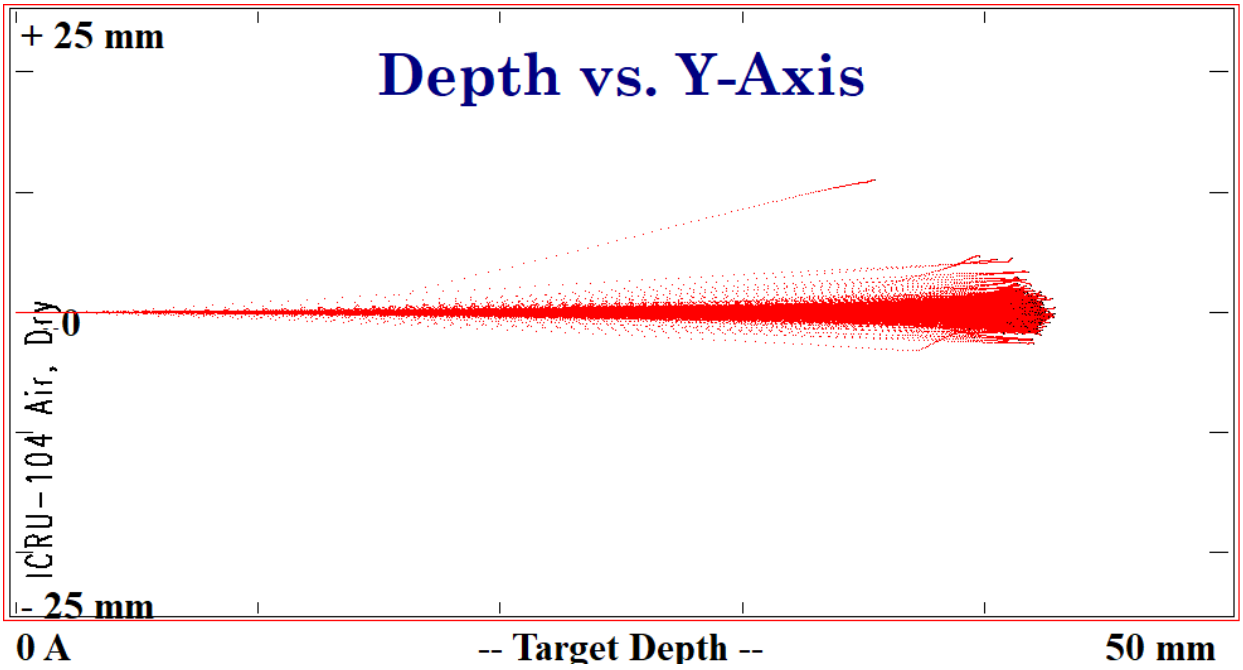

Figure 16: Depth of alpha particles in 5 cm air.

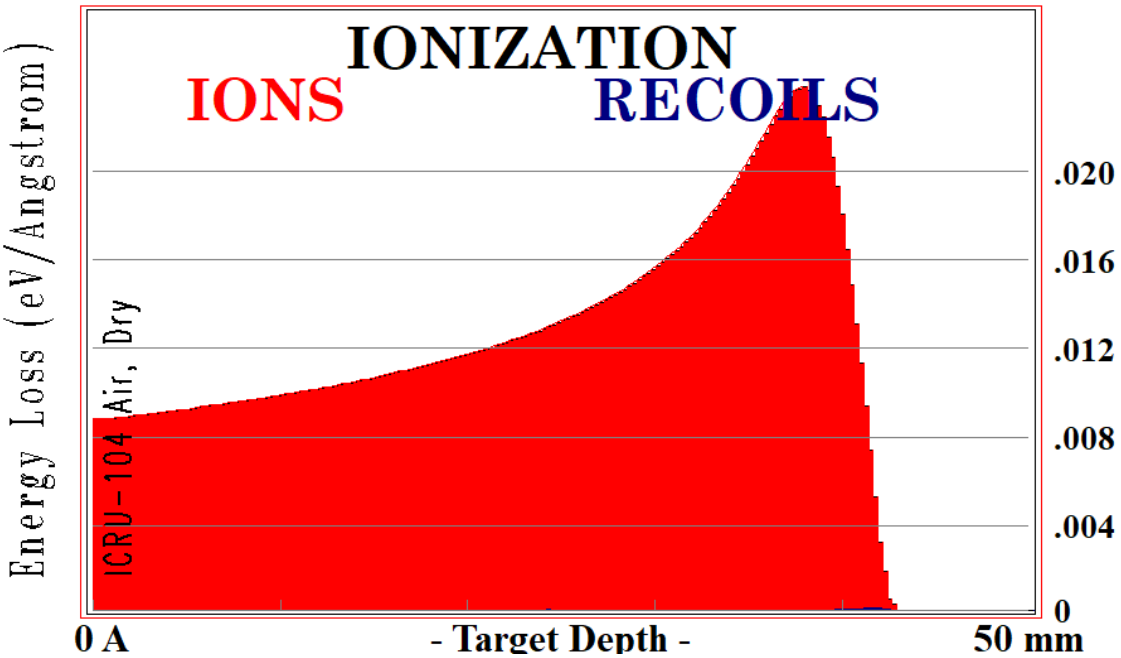

Figure 17: Bragg curve of alpha particles in 5 cm air.

From the two plots, it can be denoted that the intensity of alpha particles decreases when the distance increases. Since, alpha particles lose their energy when they interact with the particles present in the air. Here, the range of the alpha particles in air is around 3.5 to 4 cm. The Bragg peak is about 4.3 cm and beyond that, the energy decreases sharply until no more signal is detected.

Task 7: Pixel Detectors

The pixel detector is an advanced detector that works like a digital camera. Indeed, both have pixels, but they differ in shape and purpose. The flat rectangles of pixels in a digital camera are used to collect all the lights that reaches the lens. Whereas a pixel detector inside a collider is built to collect information on particles from a particular point where the particles collide. However, the basic physics behind both lies on a common ground: silicon detectors. [16]

A pixel detector has three parts: sensor (Si), electronic chip, and a USB. This detector has a high resolution and is used to register different types of radiation such as X-rays, gamma radiation, neutrons, and charged particles. Pixel detectors were originally developed for particle physics applications, but they have been slowly integrated into the fields of radiological and biomedical imaging, as well as protein crystallography with synchrotron radiation. [17]

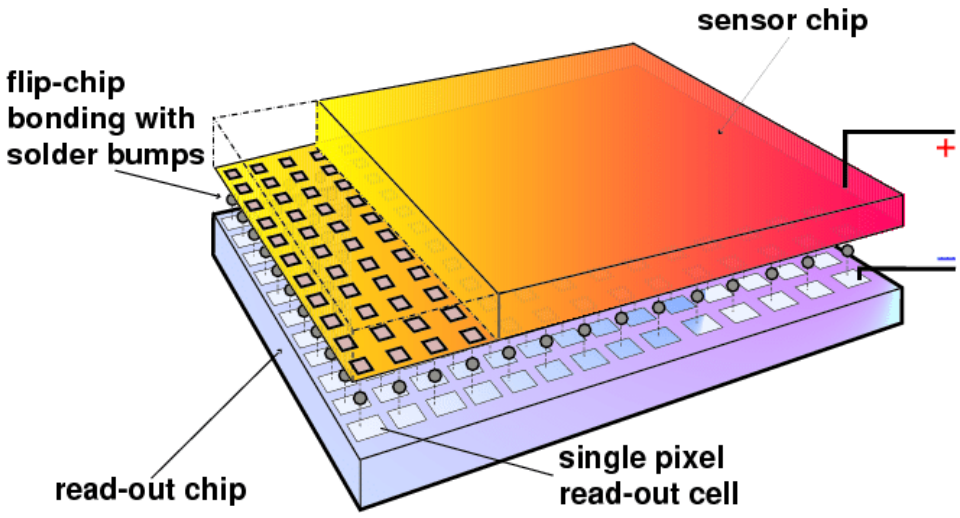

Figure 18: Schematic diagram of a hybrid pixel detector. Retrieved from: ResearchGate.

7.1. Determination of Alpha Range Particles in Air by Pixel Detectors

The range of alpha particles with (Am-241) energy about 4 MeV in air using pixel detector.

General dimensions of a pixel detector:

- Sensor size: 1.5 x 1.5 cm
- Number of pixels: 256 x 256 pixels (65,536 pixel)
- Pixel size: 55 µm x 55 µm

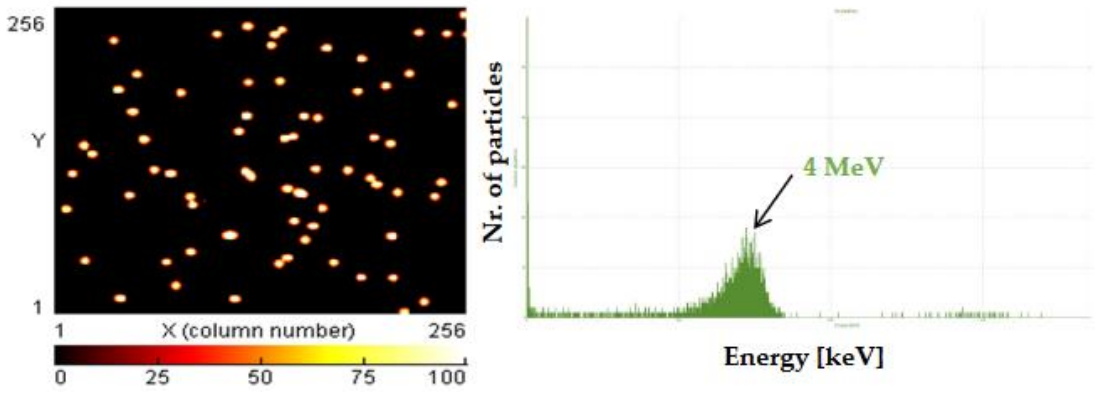

Figure 19: The range of alpha particles in air at x = 0 cm distance from the source Am-241.

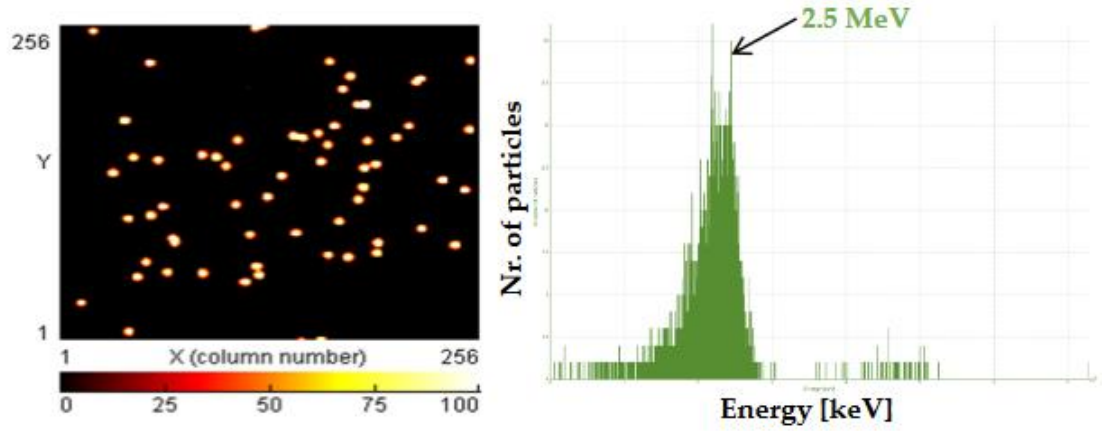

Figure 20: The range of alpha particles in air at x = 1 cm distance from the source Am-241.

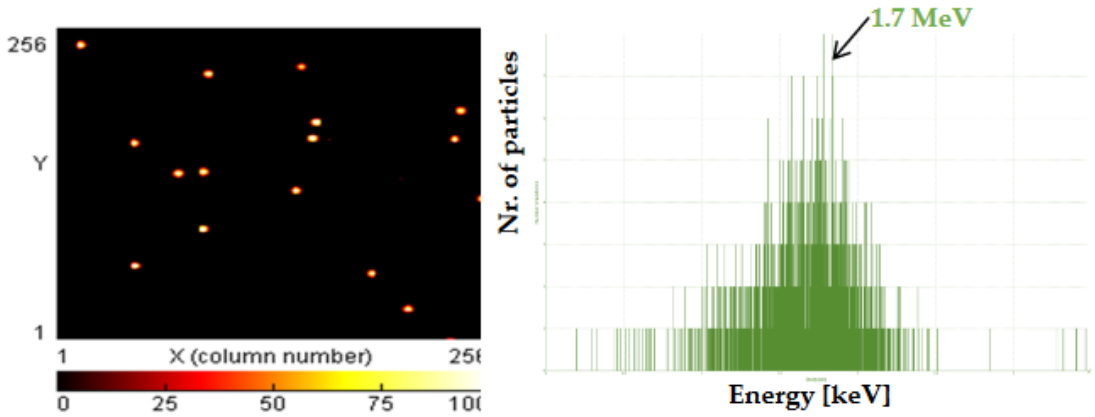

Figure 21: The range of alpha particles in air at x = 2 cm distance from the source Am-241.

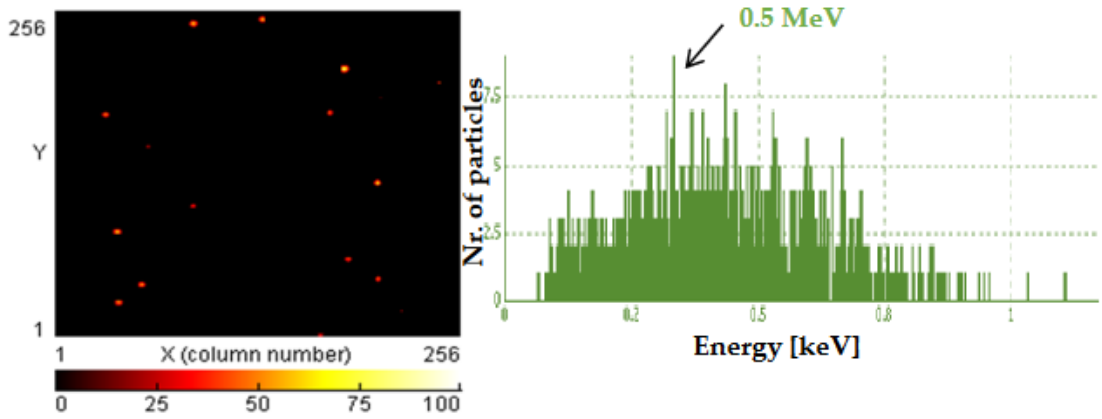

Figure 22: The range of alpha particles in air at x = 2.5 cm distance from the source Am-241.

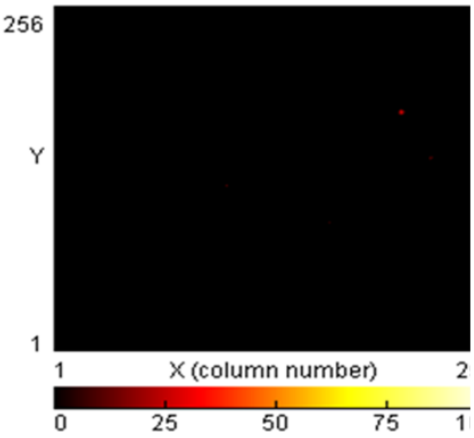

Figure 23: The range of alpha particles in air at x = 3 cm distance from the source Am-241.

At a 3 cm distance from the source, there are no alpha particles detected. Therefore, the maximum range of alpha particles in air as measured by a pixel detector is about **3 cm**.

4. Conclusions

In this project, the fundamental components of radiation protection and radiation sources are investigated. This includes the various radiation sources and types, its units and quantification, radiation protection principles, the various scintillation detectors and scintillating crystals, the components of a scintillation detector, peak integration, energy calculation and source identification, attenuation coefficient determination, and range of alpha particles in air.

Software such as ROOT, Origin Analysis, Excel, and SRIM simulation are among the programs used.

The technical specifications of the two scintillation detectors are compared through the experimental methods and outcomes. In contrast to a BGO detector, an NaI detector clearly has a better and more advantageous resolution. But each one has a unique set of characteristics and applications.

The energy of the unknown source is determined from the equation of the calibration line using a known energy. To pinpoint the source, the calculated energy is contrasted with data from the literature. It should be noted that it is only a rough estimate and may not be the source of radiation in its entirety. Due to the possibility of errors during the Gaussian fitting in ROOT, values may vary.

The attenuation coefficients of aluminum and copper are determined using the BGO detector at 2000 V and Cs-137 as the radioactive source. The reduction of an x-ray beam as it passes through matter is known as attenuation, and each material has its own attenuation coefficient. This is a critical factor in medical imaging. When the two materials are compared, copper has a higher attenuation coefficient than aluminum. Copper has a higher atomic number and density than aluminum, making it more efficient for shielding.

The range of alpha particles in air is determined using the plastic detector, SRIM simulation, and the pixel detector. It ranges from 3 to 4 cm, depending on the detector, the radioactive source, and the intensity of the energy applied.

In a nutshell, the project's primary goals have been accomplished.

Acknowledgements

This project work was made possible by the JINR INTEREST Program, Wave 8, under the supervision of Dr. Said Abou El-Azm and collaboration with the other participants.

References

1. Waste, R. (2006). IAEA Safety Standards.
2. *Unpacking Nuclear*. (2020, December 3). Retrieved from Orano Group: https://www.orano.group/en/unpacking-nuclear/all-about-radioactivity
3. Galindo, A. (2023, January 25). IAEA Newsletter. Retrieved from IAEA Org: https://www.iaea.org/newscenter/news/what-is-radiation
4. Frane N, Bitterman A. Radiation Safety and Protection. [Updated 2022 May 23]. In: StatPearls [Internet]. Treasure Island (FL): StatPearls Publishing; 2022 Jan-. Available from: https://www.ncbi.nlm.nih.gov/books/NBK557499/
5. Schauer, D. A., & Linton, O. W. (2009). NCRP report No. 160, ionizing radiation exposure of the population of the United States, medical exposure—are we doing less with more, and is there a role for health physicists?. Health physics, 97(1), 1-5.
6. United Nations Scientific Committee on the Effects of Atomic Radiation. (2017). Sources, effects and risks of ionizing radiation, united nations scientific committee on the effects of atomic radiation (UNSCEAR) 2016 report: report to the general assembly, with scientific annexes. United Nations.
7. Radiation Doses. (2020, December 22). Retrieved from Canadian Nuclear Safety Commission: http://nuclearsafety.gc.ca/eng/resources/radiation/introduction-to-radiation/radiation-doses.cfm
8. Valentin, J. (2007). The 2007 recommendations of the international commission on radiological protection (Vol. 37, No. 2-4, pp. 1-133). Oxford: Elsevier.
9. Knoll, G. F. (2010). Radiation detection and measurement. John Wiley & Sons.
10. Radiation Detection Scintillators. (2022). Retrieved from Luxium Solutions: https://www.crystals.saint-gobain.com/radiation-detection-scintillators/crystal-scintillators/bgo-bismuth-germanate#
11. Advatech-Radiation Detection/Imaging and Photonics. Retrieved from Advatech UK Limited: https://www.advatech-uk.co.uk/radiationdetectors-scint.html
12. Radiation Detection Scintillators. (2022). Retrieved from Luxium Solutions: https://www.crystals.saint-gobain.com/radiation-detection-scintillators/crystal-scintillators/naitl-scintillation-crystals#

13. G. Blasse. Chemistry of Materials 1994 6 (9), 1465-1475. DOI: 10.1021/cm00045a002. Retrieved from: web.stanford.edu/group/scintillators/links.html
14. Priamo F, Bell D, Sangheli A, et al. Linear attenuation coefficient. Reference article, Radiopaedia.org (Accessed on 15 Mar 2023) https://doi.org/10.53347/rID-31918.
15. Britannica, T. Editors of Encyclopaedia (Invalid Date). range. Encyclopedia Britannica. https://www.britannica.com/science/range-particle-radiation.
16. Quantum Diaries Organization. (2008). Retrieved from: https://www.quantumdiaries.org/2008/07/25/how-a-pixel-detector-works/
17. Wermes, N. (2005). Pixel Detectors. Retrieved from: https://cds.cern.ch/record/913132/files/p101.pdf